

On the problem of deformed spherical systems in Modified Newtonian Dynamics

Chung-Ming Ko

*Institute of Astronomy, Department of Physics and Center for Complex Systems,
National Central University, Jhongli District, Taoyuan City, Taiwan 320, R.O.C.*

cmko@astro.ncu.edu.tw

ABSTRACT

Based on Newtonian dynamics, observations show that the luminous masses of astrophysical objects that are the size of a galaxy or larger are not enough to generate the measured motions which they supposedly determine. This is typically attributed to the existence of dark matter, which possesses mass but does not radiate (or absorb radiation). Alternatively, the mismatch can be explained if the underlying dynamics is not Newtonian. Within this conceptual scheme, Modified Newtonian Dynamics (MOND) is a successful theoretical paradigm. MOND is usually expressed in terms of a nonlinear Poisson equation, which is difficult to analyse for arbitrary matter distributions. We study the MONDian gravitational field generated by slightly non-spherically symmetric mass distributions based on the fact that both Newtonian and MONDian fields are conservative (which we refer to as the compatibility condition). As the non-relativistic version of MOND has two different formulations (AQUAL and QuMOND) and the compatibility condition can be expressed in two ways, there are four approaches to the problem in total. The method involves solving a suitably defined linear deformation potential, which generally depends on the choice of MOND interpolation function. However, for some specific form of the deformation potential, the solution is independent of the interpolation function.

Subject headings: gravitation - methods: analytical - galaxies: structure - dark matter

1. Introduction

The mass of an astrophysical object can be estimated using two methods. The first one relies on the observed total amount of radiation emitted by the matter of the object and the mass measured is called the luminous mass. The second one depends on the motions of ambient objects (other objects or the object under investigation) that are affected by the matter of the object and the mass measured is called the dynamical mass. The first method requires a relation between the mass and the luminosity of the matter (either theoretical or empirical). The relation is known as the “mass-to-light ratio”. The second method assumes that we understand the dynamical law governing the motions of the objects. Newtonian dynamics (Newton’s laws of motion supplemented by Newton’s law of gravity) is well tested locally. If we apply Newtonian dynamics to astrophysical objects that are the size of a galaxy or larger, we generally find that the luminous mass is smaller than (usually much smaller than) the dynamical mass. This mismatch in mass is usually called the “missing mass problem”. A logical solution, at this scale, is that the matter is dominated by a type of matter that possesses mass (thus provides gravity) but does not emit or absorb electromagnetic radiation. This type of matter is commonly known as dark matter. We note that dark matter is also required in cosmology. For a review of the history of dark matter, the reader is referred to the book by Sanders (2010a).

However, the mismatch in mass can be (and should be) interpreted in terms of a mismatch in acceleration: the observed motion does not match the expected motion produced by the measured luminous mass if Newtonian dynamics is adopted. What if Newtonian dynamics is not correct? This will open up explanations other than dark matter for the mismatch in acceleration (or the “missing mass problem”). Milgrom (1983a) proposed that when the acceleration is small with respect to a characteristic scale (which is usually called the acceleration constant a_0), Newton’s second law of motion must be modified in order to explain the mismatch (the acceleration must be larger than that predicted by Newton’s law). In subsequent papers, Milgrom provided a natural explanation to the flat rotation curve and Tully-Fisher relation of spiral galaxies, the mass-to-light ratio of galaxy systems, etc. (Milgrom 1983b,c). This explanation was the birth of Modified Newtonian Dynamics (MOND). We note that it is the scale of acceleration that distinguishes MOND from Newtonian dynamics, not other scales such as size, etc. In the following year, Bekenstein & Milgrom (1984) put the theory in a Lagrangian formulation which can be viewed as a modified theory of gravity. Their theory is called Aquadratic Lagrangian theory (AQUAL). Milgrom (2010a) put forward another formulation of MOND called Quasi-linear formulation of MOND (QuMOND). We will discuss in detail the two formulations in Section 2. MOND has been very successful in explaining many “missing mass problems” in galaxy-scale objects, such as the flat rotation curve of spiral galaxies (e.g.,

Begeman et al. 1991; Sanders 1996; de Blok & McGaugh 1998; Sanders & Verheijen 1998; Sanders & McGaugh 2002; Famaey & Binney 2005; Milgrom 2007; Sanders 2007; Swaters et al. 2010), the baryonic Tully-Fisher relation (e.g., McGaugh 2005, 2011, 2012), velocity dispersion in elliptical galaxies (e.g., Milgrom & Sanders 2003; Chae & Gong 2015; Tian & Ko 2015), the Faber-Jackson relation (e.g., Sanders 2010b), and hot gas in elliptical galaxies (e.g., Milgrom 2012a). For the scales of cluster of galaxies, MOND is not as satisfactory. It seems that some form of dark matter is needed (see, e.g., Aguirre et al. 2001; Sanders 2003; Clowe et al. 2003; Angus & McGaugh 2008). It is interesting to note that the gravitational redshift in galaxy clusters has also been studied in MOND (Wojtak et al. 2011; Bekenstein & Sanders 2012).

Bekenstein (2004) proposed a covariant relativistic gravity theory called Tensor-Vector-Scalar theory (TeVeS) in which MOND is the non-relativistic limit. Later, Milgrom (2009a) suggested another relativistic theory for MOND called BiMOND. With a viable relativistic version of MOND, one can study relativistic phenomena such as gravitational lensing (see, e.g., Chiu et al. 2006; Zhao et al. 2006; Chiu et al. 2011; Milgrom 2013; Tian et al. 2013; Sanders 2014) and cosmology (see, e.g., Skordis 2006; Skordis et al. 2006; Dodelson & Liguori 2006; Bourliot et al. 2007; Skordis 2008, 2009; Angus 2009; Clifton & Zlosnik 2010; Milgrom 2010b). Famaey & McGaugh (2013) and McGaugh (2015) pointed out challenges to both concordance Λ CDM cosmology and that of relativistic MOND. We note that there are some theoretical issues to be sorted out in some forms of relativistic MOND theory (see, e.g., Seifert 2007; Contaldi et al. 2008; Famaey & McGaugh 2012).

Although MOND was “invented” to study systems in the small acceleration regime, a number of studies have been devoted to the high acceleration regime (i.e., regime close to the Newtonian limit), in particular, to the motion of objects in the Solar System, such as the Pioneer anomaly, perihelion precession, etc. (see, e.g., Milgrom 1983a, 2009b, 2012b; Sanders 2006; Sereno & Jetzer 2006; Iorio 2008, 2009, 2010a,b, 2013; Sokaliwska et al. 2010; Blanchet & Novak 2011; Hees et al. 2014, 2016). Precise measurements in the Solar System would place constraints on MOND (at least in the high acceleration regime). Discussions of MOND in Solar System often involve the so-called “external field effect” (EFE; Milgrom 1983a; Bekenstein & Milgrom 1984). There is an absolute acceleration scale in MOND (the acceleration constant a_0), and thus the internal dynamics may depend on the external gravitational field even if it is a uniform field (this violates the strong equivalence principle). There are three characteristic accelerations: the gravitational acceleration by the internal field and that of the external field, and the acceleration constant a_0 (hereafter gravitational field and acceleration will be used interchangeably). Roughly speaking, if either the internal field or the external field is larger than a_0 , then the internal dynamics will be governed by standard Newtonian dynamics. For those cases where a_0 is the largest, one finds the follow-

ing: (i) if the external field is larger than the internal field, then the internal dynamics will be Newtonian but with a larger “effective” Newtonian gravitational constant; (ii) if the internal field is larger than the external field, then the internal dynamics will be governed by MOND. EFE is also important in the study of the dynamics of star clusters and satellite galaxies (see, e.g., Brada & Milgrom 2000b; Baumgardt et al. 2005; Gentile et al. 2007; Haghi et al. 2009; Klypin & Prada 2009; Haghi et al. 2011; McGaugh & Milgrom 2013a,b; Derakhshani 2014; Lüghausen et al. 2014).

It is worth noting that tabletop experiments on gravitational redshift using atom interferometers (Müller et al. 2010; Hohensee et al. 2011) may be able to place some constraint on MOND in the high acceleration regime (see Appendix A).

For more details on classical MOND, relativistic MOND, and other topics related to MOND, the reader is referred to the excellent review by Famaey & McGaugh (2012) and references therein.

As a modified theory of gravity, MOND can be expressed in terms of a nonlinear Poisson equation (e.g., Bekenstein & Milgrom 1984) in which the Newtonian gravitational field and the MONDian field are related. In general, the two fields differ by the curl of a vector, i.e., a solenoidal field, which in general depends on the matter or mass distribution of the system (more on this in Section 2). As mentioned in Bekenstein & Milgrom (1984), the solenoidal field vanishes identically only if the system under investigation is highly symmetric (e.g., planar, cylindrical, spherical). For other systems, this term makes the analysis difficult and interesting. Over the years, numerical schemes or solvers have been developed to solve the Poisson equation of less symmetric systems (see, e.g., Brada & Milgrom 1999; Ciotti et al. 2006; Nipoti et al. 2007a; Tiret & Combes 2007; Feix et al. 2008; Llinares et al. 2008; Londrillo & Nipoti 2009; Angus et al. 2012; Candlish et al. 2015; Lüghausen et al. 2015). These codes enable us to study, in the framework of MOND, the structure and evolution of stellar systems (mostly accompanied by an N-Body code), such as stellar dynamics (see, e.g., Nipoti et al. 2008, 2011), disk galaxies (see, e.g., Brada & Milgrom 1999, 2000a; Tiret & Combes 2007, 2008; Angus et al. 2012; Lüghausen et al. 2015), elliptical galaxies (see, e.g., Ciotti et al. 2006; Nipoti et al. 2007a; Wu et al. 2009; Wang et al. 2008; Wu et al. 2009), satellite galaxies with an external field effect (see, e.g., Brada & Milgrom 2000b; Wu et al. 2007; Nipoti et al. 2007b; Haghi et al. 2011; Angus et al. 2014; Lüghausen et al. 2014; Candlish et al. 2015), gravitational lensing (see, e.g., Feix et al. 2008), and cosmic structure formation (see, e.g., Llinares et al. 2008).

Although the nonlinear Poisson equation is difficult to analyse analytically, some progress has been made on disk-like structures (see, e.g., Brada & Milgrom 1995) and asymmetric or triaxial structures (see, e.g., Angus et al. 2006; Ciotti et al. 2006; Shan et al. 2008;

Ciotti et al. 2012). Analytic solutions have their role in our understanding of the systems and they are useful for testing numerical schemes. This article explores analytically approximated solutions to slightly deformed spherical systems (cf. e.g., Milgrom 1986; Ciotti et al. 2006).

Both Newtonian and MONDian fields are conservative fields (i.e., expressible in terms of the gradient of a potential). Both of their curls are identically zero. We called the simultaneous curl-free requirement on both fields the compatibility condition. Making use of this compatibility condition, we put forward an approximation scheme to solve the MONDian gravitational potential. As there are two formulations of MOND (AQUAL and QuMOND) and the compatibility condition can be written in two ways, we have four approaches to the problem altogether. The paper is organized as follows. Section 2 describes the two common formulations of MOND, AQUAL and QuMOND, and their corresponding compatibility conditions. Starting from a spherical system, we present treatments for slightly deformed systems for AQUAL and QuMOND in Sections 3.1 and 3.2, respectively. A simple example is given in Section 4 for illustration. Section 5 provides some discussions and remarks.

2. Two formulations of MOND

MOND was invented as a modified law of inertia (Milgrom 1983a). Later, it was noticed that MOND can be (and is better) interpreted as a theory of modified gravity (e.g., Bekenstein & Milgrom 1984). Below, we present two formulations of MOND that were developed over the years: Quadratic Lagrangian theory (AQUAL, Bekenstein & Milgrom 1984) and Quasi-linear formulation of MOND (QuMOND, Milgrom 2010a).

2.1. AQUAL

In AQUAL formulation, the gravitational acceleration in MOND is $\mathbf{g}_A = -\nabla\Phi_A$, where the potential is given by the nonlinear Poisson equation

$$\nabla \cdot [\tilde{\mu}(x_A)\nabla\Phi_A] = 4\pi G\rho = \nabla^2\Phi_N, \quad x_A = \frac{|\nabla\Phi_A|}{a_0} = \frac{|\mathbf{g}_A|}{a_0}, \quad (1)$$

where Φ_N is the Newtonian gravitational potential. Here, a_0 is the utmost important acceleration constant of MOND. $\tilde{\mu}(x_A)$ is called the interpolation function in AQUAL, and $\tilde{\mu}(x_A) \rightarrow 1$ as $x_A \rightarrow \infty$, and $\tilde{\mu}(x_A) \rightarrow x_A$ as $x \rightarrow 0$ (i.e., Newtonian regime and deep MOND regime, respectively). Different forms of the interpolation function have been used in the literature. The most commonly used forms are, e.g., the standard form proposed by Milgrom

(1983a),

$$\tilde{\mu}(x_A) = \frac{x_A}{\sqrt{1+x_A^2}}, \quad (2)$$

the simple form by Famaey & Binney (2005),

$$\tilde{\mu}(x_A) = \frac{x_A}{(1+x_A)}, \quad (3)$$

and the Bekenstein form by Bekenstein (2004),

$$\tilde{\mu}(x_A) = \frac{-1 + \sqrt{1+4x_A}}{1 + \sqrt{1+4x_A}}. \quad (4)$$

All of these forms (and some others in the literature) can be included in the two-parameter canonical form proposed by Chiu et al. (2011):

$$\tilde{\mu}(x_A) = \left[1 - \frac{2}{(1+\eta x_A^\alpha) + \sqrt{(1-\eta x_A^\alpha)^2 + 4x_A^\alpha}} \right]^{1/\alpha}, \quad (5)$$

where $\alpha > 0$ and $\eta \geq 0$. Here, $(\alpha, \eta) = (1, 0)$, $(1, 1)$, and $(2, 1)$ correspond to the Bekenstein form, the simple form, and the standard form, respectively.

Integrating Equation (1) once gives

$$\tilde{\mu}(x_A) \mathbf{g}_A = -\tilde{\mu}(x_A) \nabla \Phi_A = -\nabla \Phi_N + \nabla \times \mathbf{h} = \mathbf{g}_N + \nabla \times \mathbf{h} = \mathbf{G}_N, \quad (6)$$

where $\mathbf{g}_N = -\nabla \Phi_N$ is the Newtonian gravitational acceleration. Here, \mathbf{h} is an arbitrary vector. Inverting Equation (6) gives

$$-\nabla \Phi_A = \mathbf{g}_A = \tilde{\nu}(\chi_N) \mathbf{G}_N = \tilde{\nu}(\chi_N) (\mathbf{g}_N + \nabla \times \mathbf{h}) = \tilde{\nu}(\chi_N) (-\nabla \Phi_N + \nabla \times \mathbf{h}), \quad (7)$$

where

$$\chi_N = \frac{|\mathbf{G}_N|}{a_0} = \frac{1}{a_0} |\mathbf{g}_N + \nabla \times \mathbf{h}| = \frac{1}{a_0} |-\nabla \Phi_N + \nabla \times \mathbf{h}|. \quad (8)$$

$\tilde{\nu}(\chi_N)$ is called the inverted interpolation function in AQUAL. The inverted form corresponding to the canonical form of Equation (5) is (Chiu et al. 2011)

$$\tilde{\nu}(\chi_N) = \left[1 + \frac{1}{2} \left(\sqrt{4\chi_N^{-\alpha} + \eta^2} - \eta \right) \right]^{1/\alpha}. \quad (9)$$

Since \mathbf{g}_A and \mathbf{g}_N can be expressed as a gradient of a potential, there exists a compatibility condition for Equations (6) and (7). Taking the curl of Equation (6) gives

$$0 = \nabla \times \mathbf{g}_N = \nabla \times (\tilde{\mu} \mathbf{g}_A) - \nabla \times \nabla \times \mathbf{h} = \frac{1}{a_0} \frac{d\tilde{\mu}}{dx_A} (\nabla |\mathbf{g}_A|) \times \mathbf{g}_A - \nabla \times \nabla \times \mathbf{h}, \quad (10)$$

and taking the curl of Equation (7) gives

$$0 = \nabla \times \mathbf{g}_A = \nabla \times (\tilde{\nu} \mathbf{G}_N) = \frac{1}{a_0} \frac{d\tilde{\nu}}{d\chi_N} (\nabla |\mathbf{G}_N|) \times \mathbf{G}_N + \tilde{\nu} \nabla \times \mathbf{G}_N. \quad (11)$$

For highly symmetric systems (such as, planar, cylindrical, spherical), $\nabla \times \mathbf{h} = 0$. Consequently, $\chi_N = x_N = |\mathbf{g}_N|/a_0$,

$$\tilde{\mu}(x_A) \mathbf{g}_A = \mathbf{g}_N, \quad \mathbf{g}_A = \tilde{\nu}(x_N) \mathbf{g}_N. \quad (12)$$

and the compatibility conditions, Equations (10) and (11), are satisfied automatically.

2.2. QuMOND

In QuMOND formulation, the gravitational acceleration in MOND is $\mathbf{g}_Q = -\nabla \Phi_Q$, where the potential is given by

$$\nabla^2 \Phi_Q = \nabla \cdot [\nu(x_N) \nabla \Phi_N], \quad \nabla^2 \Phi_N = 4\pi G \rho, \quad x_N = \frac{|\nabla \Phi_N|}{a_0} = \frac{|\mathbf{g}_N|}{a_0}. \quad (13)$$

$\nu(x_N)$ is called the inverted interpolation function in QuMOND, and $\nu(x_N) \rightarrow 1$ as $x_N \rightarrow \infty$, and $\nu(x_N) \rightarrow 1/\sqrt{x_N}$ as $x_N \rightarrow 0$ (i.e., Newtonian regime and deep MOND regime, respectively). A useful form for the inverted interpolation function is Equation (9) (with χ_N replaced by x_N).

Integrating Equation (13) once gives

$$\nu(x_N) \mathbf{g}_N = -\nu(x_N) \nabla \Phi_N = -\nabla \Phi_Q - \nabla \times \mathbf{A} = \mathbf{g}_Q - \nabla \times \mathbf{A} = \mathbf{G}_Q. \quad (14)$$

Here, \mathbf{A} is an arbitrary vector. Inverting Equation (14) gives (cf. Equation (6))

$$-\nabla \Phi_N = \mathbf{g}_N = \mu(\chi_Q) \mathbf{G}_Q = \mu(\chi_Q) (\mathbf{g}_Q - \nabla \times \mathbf{A}) = \mu(\chi_Q) (-\nabla \Phi_Q - \nabla \times \mathbf{A}), \quad (15)$$

where (cf. Equation (8))

$$\chi_Q = \frac{|\mathbf{G}_Q|}{a_0} = \frac{1}{a_0} |\mathbf{g}_Q - \nabla \times \mathbf{A}| = \frac{1}{a_0} |-\nabla \Phi_Q - \nabla \times \mathbf{A}|. \quad (16)$$

$\mu(\chi_Q)$ is called the interpolation function in QuMOND. A useful form for the interpolation function is Equation (5) (with x_A replaced by χ_Q).

Similar to AQUAL, there exists a compatibility condition for Equations (14) and (15). Taking the curl of Equation (14) gives (cf. Equation (10))

$$0 = \nabla \times \mathbf{g}_Q = \nabla \times (\nu \mathbf{g}_N) + \nabla \times \nabla \times \mathbf{A} = \frac{1}{a_0} \frac{d\nu}{dx_N} (\nabla |\mathbf{g}_N|) \times \mathbf{g}_N + \nabla \times \nabla \times \mathbf{A}, \quad (17)$$

and taking the curl of Equation (15) gives (cf. Equation (11))

$$0 = \nabla \times \mathbf{g}_N = \nabla \times (\mu \mathbf{G}_Q) = \frac{1}{a_0} \frac{d\mu}{d\chi_Q} (\nabla |\mathbf{G}_Q|) \times \mathbf{G}_Q + \mu \nabla \times \mathbf{G}_Q. \quad (18)$$

Similar to AQUAL, for highly symmetric systems (such as, planar, cylindrical, spherical), $\nabla \times \mathbf{A} = 0$. Consequently, $\chi_Q = x_Q = |\mathbf{g}_Q|/a_0$,

$$\nu(x_N) \mathbf{g}_N = \mathbf{g}_Q, \quad \mathbf{g}_N = \mu(x_Q) \mathbf{g}_Q. \quad (19)$$

and the compatibility conditions, Equations (17) and (18), are satisfied automatically.

3. Systems slightly deformed from spherical symmetry

To find the MONDian gravitational acceleration produced by a general mass distribution ρ is a formidable task. One has to solve $\nabla \cdot [\tilde{\mu}(|\mathbf{g}_A|/a_0) \mathbf{g}_A] = \nabla \cdot \mathbf{g}_N$ in AQUAL formulation or $\nabla \cdot \mathbf{g}_Q = \nabla \cdot [\nu(|\mathbf{g}_N|/a_0) \mathbf{g}_N]$ in QuMOND formulation, with the Newtonian gravitational acceleration given by $\nabla \cdot \mathbf{g}_N = -4\pi G\rho$. However, for a spherical mass distribution $\rho(r)$, the solution can be written down as follows. The Newtonian gravitational acceleration is given by

$$\mathbf{g}_N = -\frac{Gm(r)}{r^2} \hat{\mathbf{e}}_r, \quad m(r) = \int_0^r 4\pi \rho(r') dr'. \quad (20)$$

Here, $m(r)$ is the mass within radius r . The MONDian gravitational acceleration is given by $\mathbf{g}_A = \tilde{\nu}(|\mathbf{g}_N/a_0|) \mathbf{g}_N$ in AQUAL formulation and $\mathbf{g}_Q = \nu(|\mathbf{g}_N/a_0|) \mathbf{g}_N$ in QuMOND formulation (provided that the interpolation function $\tilde{\nu}$ and ν are known). The compatibility conditions mentioned in Section 2 are satisfied automatically.

Base on the spherical solution, we propose a treatment for slightly deformed spherical systems. Our goal is to find solutions that will at least approximately satisfy the compatibility condition. Since we can express the compatibility condition in terms of the interpolation function ($\tilde{\mu}$ in AQUAL or μ in QuMOND) or its inverse ($\tilde{\nu}$ in AQUAL or ν in QuMOND), we have four schemes: Equation (11) and (10) for AQUAL and Equations (17) and (18) for QuMOND, respectively. We present the four schemes in detail in the following. We note that on the one hand, AQUAL and MOND are not exactly equivalent (except for the spherical, cylindrical, planar cases). On the other hand, choosing an interpolation function or its inverse is a matter of convenience.

3.1. Treatment in AQUAL

There are two expressions for the compatibility condition. We thus have two schemes: AQUAL I based on $\nabla \times \mathbf{g}_A = \nabla \times [\tilde{\nu}(\mathbf{g}_N + \nabla \times \mathbf{h})] = 0$ (Equation (7)), and AQUAL II based on $\nabla \times \mathbf{g}_N = \nabla \times (\tilde{\mu}\mathbf{g}_A - \nabla \times \mathbf{h}) = 0$ (Equation (6)).

$$3.1.1. \quad \text{AQUAL I: } \nabla \times \mathbf{g}_A = \nabla \times [\tilde{\nu}(\mathbf{g}_N + \nabla \times \mathbf{h})] = 0$$

Suppose the Newtonian gravitational acceleration deviates slightly from spherical symmetry:

$$\mathbf{g}_N = g_N^{(0)} \hat{\mathbf{e}}_r + \epsilon \mathbf{g}_N^{(1)} + \mathcal{O}(\epsilon^2), \quad (21)$$

where ϵ is the small parameter keeping track of the order, $g_N^{(0)} = g_N^{(0)}(r)$ depends on r only, and $\mathbf{g}_N^{(1)} = \mathbf{g}_N^{(1)}(r, \theta, \phi)$ depends on (r, θ, ϕ) . Since for a spherically symmetric system $\nabla \times \mathbf{h} = 0$, we expect $\nabla \times \mathbf{h} = \mathcal{O}(\epsilon)$ in slightly deformed spherical systems (i.e., non-spherical), and we replace it by $\epsilon \nabla \times \mathbf{h}_N^{(1)}$. Thus, Equation (6) becomes

$$\mathbf{G}_N = g_N^{(0)} \hat{\mathbf{e}}_r + \epsilon \left[\mathbf{g}_N^{(1)} + \nabla \times \mathbf{h}_N^{(1)} \right] + \mathcal{O}(\epsilon^2) = g_N^{(0)} \hat{\mathbf{e}}_r + \epsilon \mathbf{F}_N^{(1)} + \mathcal{O}(\epsilon^2). \quad (22)$$

Therefore, up to $\mathcal{O}(\epsilon)$, the compatibility condition Equation (11) becomes

$$0 = \tilde{\mathcal{A}}^{(0)} \left[g_N^{(0)} \nabla F_{Nr}^{(1)} - \frac{dg_N^{(0)}}{dr} \mathbf{F}_N^{(1)} \right] \times \hat{\mathbf{e}}_r + \nabla \times \mathbf{F}_N^{(1)}, \quad \tilde{\mathcal{A}}^{(0)} = \left[\frac{1}{a_0 \tilde{\nu}} \frac{d\tilde{\nu}}{d\chi_N} \right]^{(0)}. \quad (23)$$

Here, $[\cdot]^{(0)}$ denotes quantities of $\mathcal{O}(1)$ (note $a_0 \chi_N = g_N^{(0)} + \mathcal{O}(\epsilon)$), i.e., evaluated at the spherically symmetric level. Hence, $\tilde{\mathcal{A}}^{(0)} = \tilde{\mathcal{A}}^{(0)}(r)$ depends on r only. Solving Equation (23) implies that $\mathbf{F}_N^{(1)}$ can be expressed in terms of a “deformation potential” $\Psi_N^{(1)}(r, \theta, \phi)$,

$$\mathbf{F}_N^{(1)} = -\nabla \Psi_N^{(1)} + f_N^{(1)} \hat{\mathbf{e}}_r, \quad f_N^{(1)} = \frac{\tilde{\mathcal{A}}^{(0)}}{[\tilde{\mathcal{A}}^{(0)} g_N^{(0)} + 1]} \left[g_N^{(0)} \frac{\partial \Psi_N^{(1)}}{\partial r} - \frac{dg_N^{(0)}}{dr} \Psi_N^{(1)} \right]. \quad (24)$$

By the Helmholtz theorem, we can express $f_N^{(1)} \hat{\mathbf{e}}_r = -\nabla \varphi_N^{(1)} + \nabla \times \mathbf{h}_N^{(1)}$, with

$$\varphi_N^{(1)} = \int_V \frac{\nabla' \cdot [f_N^{(1)}(\mathbf{x}') \hat{\mathbf{e}}_{r'}]}{4\pi |\mathbf{x} - \mathbf{x}'|} d^3 x' - \oint_S \frac{[f_N^{(1)}(\mathbf{x}') \hat{\mathbf{e}}_{r'}] \cdot \hat{\mathbf{n}}'}{4\pi |\mathbf{x} - \mathbf{x}'|} d^2 x', \quad (25)$$

$$\mathbf{h}_N^{(1)} = \int_V \frac{\nabla' \times [f_N^{(1)}(\mathbf{x}') \hat{\mathbf{e}}_{r'}]}{4\pi |\mathbf{x} - \mathbf{x}'|} d^3 x' + \oint_S \frac{[f_N^{(1)}(\mathbf{x}') \hat{\mathbf{e}}_{r'}] \times \hat{\mathbf{n}}'}{4\pi |\mathbf{x} - \mathbf{x}'|} d^2 x'. \quad (26)$$

If the $f_N^{(1)}$ decay rapid enough as $|\mathbf{x}'|$ tends to infinity, then as the integral is extended to the entire space, the surface terms will vanish. The relation between $\mathbf{F}_N^{(1)}$ and $\mathbf{g}_N^{(1)}$ (Equation (22))

gives

$$\mathbf{g}_N = g_N^{(0)} \hat{\mathbf{e}}_r - \epsilon \nabla \left[\Psi_N^{(1)} + \varphi_N^{(1)} \right] + \mathcal{O}(\epsilon^2), \quad (27)$$

Moreover, Equation (22) gives

$$|\mathbf{G}_N| = a_0 \chi_N = a_0 \left[\chi_N^{(0)} + \epsilon \chi_N^{(1)} + \mathcal{O}(\epsilon^2) \right] = g_N^{(0)} + \epsilon F_{Nr}^{(1)} + \mathcal{O}(\epsilon^2), \quad (28)$$

and

$$\tilde{\nu}(\chi_N) = \tilde{\nu}^{(0)} + \epsilon \tilde{\nu}^{(0)} \tilde{\mathcal{A}}^{(0)} a_0 \chi_N^{(1)} + \mathcal{O}(\epsilon^2) = \tilde{\nu}^{(0)} + \epsilon \tilde{\nu}^{(0)} \tilde{\mathcal{A}}^{(0)} F_{Nr}^{(1)} + \mathcal{O}(\epsilon^2), \quad (29)$$

where $\tilde{\nu}^{(0)} = \tilde{\nu}(\chi_N^{(0)})$. Hence,

$$\mathbf{g}_A = \tilde{\nu}^{(0)} g_N^{(0)} \hat{\mathbf{e}}_r - \epsilon \tilde{\nu}^{(0)} \left[\nabla \Psi_N^{(1)} + \tilde{\mathcal{A}}^{(0)} \frac{dg_N^{(0)}}{dr} \Psi_N^{(1)} \hat{\mathbf{e}}_r \right] + \mathcal{O}(\epsilon^2). \quad (30)$$

The mass distribution is given by the Poisson equation $4\pi G\rho = \nabla \cdot \mathbf{g}_N$. If we express $\rho = \rho^{(0)}(r) + \epsilon \rho^{(1)}(r, \theta, \phi) + \mathcal{O}(\epsilon^2)$ and make use of Equations (27) and (24) (and $f_N^{(1)} \hat{\mathbf{e}}_r = -\nabla \varphi_N^{(1)} + \nabla \times \mathbf{h}_N^{(1)}$), then we obtain

$$4\pi G\rho^{(0)} = -\frac{1}{r^2} \frac{\partial r^2 g_N^{(0)}}{\partial r}, \quad (31)$$

and

$$4\pi G\rho^{(1)} = \nabla^2 \Psi_N^{(1)} - \frac{1}{r^2} \frac{\partial}{\partial r} \left\{ \frac{r^2 \tilde{\mathcal{A}}^{(0)}}{[\tilde{\mathcal{A}}^{(0)} g_N^{(0)} + 1]} \left[g_N^{(0)} \frac{\partial \Psi_N^{(1)}}{\partial r} - \frac{dg_N^{(0)}}{dr} \Psi_N^{(1)} \right] \right\}. \quad (32)$$

3.1.2. AQUAL II: $\nabla \times \mathbf{g}_N = \nabla \times (\tilde{\mu} \mathbf{g}_A - \nabla \times \mathbf{h}) = 0$

Suppose the MONDian gravitational acceleration deviates slightly from spherical symmetry:

$$\mathbf{g}_A = g_A^{(0)} \hat{\mathbf{e}}_r + \epsilon \mathbf{g}_A^{(1)} + \mathcal{O}(\epsilon^2) = g_A^{(0)} \hat{\mathbf{e}}_r - \epsilon \nabla \Phi_A^{(1)} + \mathcal{O}(\epsilon^2). \quad (33)$$

Here, $g_A^{(0)} = g_A^{(0)}(r)$ depends on r only, $\mathbf{g}_A^{(1)} = \mathbf{g}_A^{(1)}(r, \theta, \phi)$ depends on (r, θ, ϕ) , and $\Phi_A^{(1)}(r, \theta, \phi)$ can be called the ‘‘deformation potential’’. Besides, we expect $\nabla \times \mathbf{h} = \mathcal{O}(\epsilon)$ in slightly non-spherical systems because $\nabla \times \mathbf{h} = 0$ for spherical systems. We replace the curl term by $\epsilon \nabla \times \mathbf{h}_A^{(1)}$.

Up to $\mathcal{O}(\epsilon)$, the compatibility condition (Equation (10)) becomes

$$0 = \tilde{\mu}^{(0)} \tilde{\mathcal{B}}^{(0)} \left[g_A^{(0)} \nabla g_{Ar}^{(1)} - \frac{dg_A^{(0)}}{dr} \mathbf{g}_A^{(1)} \right] \times \hat{\mathbf{e}}_r - \nabla \times \nabla \times \mathbf{h}_A^{(1)}, \quad \tilde{\mathcal{B}}^{(0)} = \left[\frac{1}{a_0 \tilde{\mu}} \frac{d\tilde{\mu}}{dx_A} \right]^{(0)}. \quad (34)$$

Here, $[\cdot]^{(0)}$ denotes quantities of $\mathcal{O}(1)$ (note $a_0 x_A = g_A^{(0)} + \mathcal{O}(\epsilon)$), i.e., evaluated at the spherically symmetric level. Hence, $\tilde{\mathcal{B}}^{(0)} = \tilde{\mathcal{B}}^{(0)}(r)$ depends on r only. Solving Equation (34) with $\mathbf{g}_A^{(1)} = -\nabla\Phi_A^{(1)}$ implies that

$$q_A^{(1)} \hat{\mathbf{e}}_r = -\nabla\Upsilon_A^{(1)} - \nabla \times \nabla \times \mathbf{h}_A^{(1)}, \quad q_A^{(1)} = \tilde{\mu}^{(0)} \tilde{\mathcal{B}}^{(0)} \left[g_A^{(0)} \frac{\partial \Phi_A^{(1)}}{\partial r} - \frac{d g_A^{(0)}}{dr} \Phi_A^{(1)} \right]. \quad (35)$$

The Helmholtz theorem gives

$$\Upsilon_A^{(1)} = \int_V \frac{\nabla' \cdot [q_A^{(1)}(\mathbf{x}') \hat{\mathbf{e}}_{r'}]}{4\pi|\mathbf{x} - \mathbf{x}'|} d^3x' - \oint_S \frac{[q_A^{(1)}(\mathbf{x}') \hat{\mathbf{e}}_{r'}] \cdot \hat{\mathbf{n}}'}{4\pi|\mathbf{x} - \mathbf{x}'|} d^2x', \quad (36)$$

$$\mathbf{h}_A^{(1)} = - \int_V \frac{\nabla' \times [q_A^{(1)}(\mathbf{x}') \hat{\mathbf{e}}_{r'}]}{4\pi|\mathbf{x} - \mathbf{x}'|} d^3x' - \oint_S \frac{[q_A^{(1)}(\mathbf{x}') \hat{\mathbf{e}}_{r'}] \times \hat{\mathbf{n}}'}{4\pi|\mathbf{x} - \mathbf{x}'|} d^2x'. \quad (37)$$

If $q_A^{(1)}$ decay rapidly enough as $|\mathbf{x}'|$ tends to infinity, then as the integral is extended to the entire space, the surface terms will vanish.

Note that

$$\tilde{\mu}(x_A) \mathbf{g}_A = \tilde{\mu}^{(0)} g_A^{(0)} \hat{\mathbf{e}}_r - \epsilon \tilde{\mu}^{(0)} \left[\nabla \Phi_A^{(1)} + \tilde{\mathcal{B}}^{(0)} g_A^{(0)} \frac{\partial \Phi_A^{(1)}}{\partial r} \hat{\mathbf{e}}_r \right] + \mathcal{O}(\epsilon^2), \quad (38)$$

and thus

$$\begin{aligned} \mathbf{g}_N &= \tilde{\mu}^{(0)} g_A^{(0)} \hat{\mathbf{e}}_r + \epsilon \left\{ \tilde{\mu}^{(0)} \left[\mathbf{g}_A^{(1)} + \tilde{\mathcal{B}}^{(0)} g_A^{(0)} g_{Ar}^{(1)} \hat{\mathbf{e}}_r \right] - \nabla \times \mathbf{h}_A^{(1)} \right\} + \mathcal{O}(\epsilon^2) \\ &= \tilde{\mu}^{(0)} g_A^{(0)} \hat{\mathbf{e}}_r - \epsilon \left\{ \tilde{\mu}^{(0)} \left[\nabla \Phi_A^{(1)} + \tilde{\mathcal{B}}^{(0)} \frac{d g_A^{(0)}}{dr} \Phi_A^{(1)} \hat{\mathbf{e}}_r \right] - \nabla \Upsilon_A^{(1)} \right\} + \mathcal{O}(\epsilon^2). \end{aligned} \quad (39)$$

Equation (38) or (39) gives the mass distribution

$$4\pi G \rho^{(0)} = -\frac{1}{r^2} \frac{\partial r^2 g_N^{(0)}}{\partial r} = -\frac{1}{r^2} \frac{\partial r^2 \tilde{\mu}^{(0)} g_A^{(0)}}{\partial r}, \quad (40)$$

and

$$4\pi G \rho^{(1)} = \nabla \cdot \left\{ \tilde{\mu}^{(0)} \left[\nabla \Phi_A^{(1)} + \tilde{\mathcal{B}}^{(0)} g_A^{(0)} \frac{d \Phi_A^{(1)}}{dr} \hat{\mathbf{e}}_r \right] \right\}. \quad (41)$$

3.2. Treatment in QuMOND

Similar to AQUAL, there are two expressions for the compatibility condition, and hence we also have two schemes: QuMOND I based on $\nabla \times \mathbf{g}_N = \nabla \times [\mu(\mathbf{g}_Q - \nabla \times \mathbf{A})] = 0$ (Equation (15)) and QuMOND II based on $\nabla \times \mathbf{g}_Q = \nabla \times (\nu \mathbf{g}_N + \nabla \times \mathbf{A}) = 0$ (Equation (14)).

$$3.2.1. \quad \text{QuMOND I: } \nabla \times \mathbf{g}_N = \nabla \times [\mu (\mathbf{g}_Q - \nabla \times \mathbf{A})] = 0$$

The mathematical procedure is the same as in Section 3.1.1. All we need to do is to change \mathbf{g}_N to \mathbf{g}_Q , \mathbf{h} to $-\mathbf{A}$, $\tilde{\nu}$ to μ , etc. We start from

$$\mathbf{g}_Q = g_Q^{(0)} \hat{\mathbf{e}}_r + \epsilon \mathbf{g}_Q^{(1)} + \mathcal{O}(\epsilon^2), \quad (42)$$

and get

$$\mathbf{G}_Q = g_Q^{(0)} \hat{\mathbf{e}}_r + \epsilon \left[\mathbf{g}_Q^{(1)} - \nabla \times \mathbf{A}_Q^{(1)} \right] + \mathcal{O}(\epsilon^2) = g_Q^{(0)} \hat{\mathbf{e}}_r + \epsilon \mathbf{F}_Q^{(1)} + \mathcal{O}(\epsilon^2). \quad (43)$$

The compatibility condition Equation (18) becomes

$$0 = \mathcal{B}^{(0)} \left[g_Q^{(0)} \nabla F_{Qr}^{(1)} - \frac{dg_Q^{(0)}}{dr} \mathbf{F}_Q^{(1)} \right] \times \hat{\mathbf{e}}_r + \nabla \times \mathbf{F}_Q^{(1)}, \quad \mathcal{B}^{(0)} = \left[\frac{1}{a_0 \mu} \frac{d\mu}{d\chi_Q} \right]^{(0)}. \quad (44)$$

Solving Equation (44) implies that $\mathbf{F}_Q^{(1)}$ can be expressed in terms of a “deformation potential” $\Psi_Q^{(1)}(r, \theta, \phi)$,

$$\mathbf{F}_Q^{(1)} = -\nabla \Psi_Q^{(1)} + f_Q^{(1)} \hat{\mathbf{e}}_r, \quad f_Q^{(1)} = \frac{\mathcal{B}^{(0)}}{[\mathcal{B}^{(0)} g_Q^{(0)} + 1]} \left[g_Q^{(0)} \frac{\partial \Psi_Q^{(1)}}{\partial r} - \frac{dg_Q^{(0)}}{dr} \Psi_Q^{(1)} \right]. \quad (45)$$

Using the Helmholtz theorem, we can express $f_Q^{(1)} \hat{\mathbf{e}}_r = -\nabla \varphi_Q^{(1)} - \nabla \times \mathbf{A}_Q^{(1)}$, with

$$\varphi_Q^{(1)} = \int_V \frac{\nabla' \cdot [f_Q^{(1)}(\mathbf{x}') \hat{\mathbf{e}}_{r'}]}{4\pi |\mathbf{x} - \mathbf{x}'|} d^3 x' - \oint_S \frac{[f_Q^{(1)}(\mathbf{x}') \hat{\mathbf{e}}_{r'}] \cdot \hat{\mathbf{n}}'}{4\pi |\mathbf{x} - \mathbf{x}'|} d^2 x', \quad (46)$$

$$\mathbf{A}_Q^{(1)} = - \int_V \frac{\nabla' \times [f_Q^{(1)}(\mathbf{x}') \hat{\mathbf{e}}_{r'}]}{4\pi |\mathbf{x} - \mathbf{x}'|} d^3 x' - \oint_S \frac{[f_Q^{(1)}(\mathbf{x}') \hat{\mathbf{e}}_{r'}] \times \hat{\mathbf{n}}'}{4\pi |\mathbf{x} - \mathbf{x}'|} d^2 x'. \quad (47)$$

If $f_Q^{(1)}$ decay rapidly enough as $|\mathbf{x}'|$ tends to infinity, then as the integral is extended to the entire space, the surface terms will vanish.

Consequently, we have

$$\mathbf{g}_Q = g_Q^{(0)} \hat{\mathbf{e}}_r - \epsilon \nabla \left[\Psi_Q^{(1)} + \varphi_Q^{(1)} \right] + \mathcal{O}(\epsilon^2), \quad (48)$$

$$\mathbf{g}_N = \mu^{(0)} g_Q^{(0)} \hat{\mathbf{e}}_r - \epsilon \mu^{(0)} \left[\nabla \Psi_Q^{(1)} + \mathcal{B}^{(0)} \frac{dg_Q^{(0)}}{dr} \Psi_Q^{(1)} \hat{\mathbf{e}}_r \right] + \mathcal{O}(\epsilon^2). \quad (49)$$

The mass distribution is

$$4\pi G \rho^{(0)} = - \frac{1}{r^2} \frac{\partial r^2 g_N^{(0)}}{\partial r} = - \frac{1}{r^2} \frac{\partial r^2 \mu^{(0)} g_Q^{(0)}}{\partial r}, \quad (50)$$

and

$$4\pi G \rho^{(1)} = \nabla \cdot \left\{ \mu^{(0)} \left[\nabla \Psi_Q^{(1)} + \mathcal{B}^{(0)} \frac{dg_Q^{(0)}}{dr} \Psi_Q^{(1)} \hat{\mathbf{e}}_r \right] \right\}. \quad (51)$$

3.2.2. *QuMOND II*: $\nabla \times \mathbf{g}_Q = \nabla \times (\nu \mathbf{g}_N + \nabla \times \mathbf{A}) = 0$

Once again, the mathematical procedure is the same as in Section 3.1.2. All we need to do is to change \mathbf{g}_A to \mathbf{g}_N , \mathbf{h} to $-\mathbf{A}$, $\tilde{\mu}$ to ν , etc. We start from

$$\mathbf{g}_N = g_N^{(0)} \hat{\mathbf{e}}_r + \epsilon \mathbf{g}_N^{(1)} + \mathcal{O}(\epsilon^2) = g_N^{(0)} \hat{\mathbf{e}}_r - \epsilon \nabla \Phi_N^{(1)} + \mathcal{O}(\epsilon^2), \quad (52)$$

where $\Phi_N^{(1)}(r, \theta, \phi)$ can be called the “deformation potential”. The compatibility condition (Equation (17)) becomes

$$0 = \nu^{(0)} \mathcal{A}^{(0)} \left[g_N^{(0)} \nabla g_{Nr}^{(1)} - \frac{dg_N^{(0)}}{dr} \mathbf{g}_N^{(1)} \right] \times \hat{\mathbf{e}}_r + \nabla \times \nabla \times \mathbf{A}_N^{(1)}, \quad \mathcal{A}^{(0)} = \left[\frac{1}{a_0 \nu} \frac{d\nu}{dx_N} \right]^{(0)}. \quad (53)$$

Solving Equation (53) implies

$$q_N^{(1)} \hat{\mathbf{e}}_r = \nabla \Upsilon_N^{(1)} + \nabla \times \mathbf{A}_N^{(1)}, \quad q_N^{(1)} = \nu^{(0)} \mathcal{A}^{(0)} \left[g_N^{(0)} \frac{\partial \Phi_N^{(1)}}{\partial r} - \frac{dg_N^{(0)}}{dr} \Phi_N^{(1)} \right], \quad (54)$$

and by the Helmholtz theorem

$$\Upsilon_N^{(1)} = - \int_V \frac{\nabla' \cdot [q_N^{(1)}(\mathbf{x}') \hat{\mathbf{e}}_{r'}]}{4\pi |\mathbf{x} - \mathbf{x}'|} d^3x' + \oint_S \frac{[q_N^{(1)}(\mathbf{x}') \hat{\mathbf{e}}_{r'}] \cdot \hat{\mathbf{n}}'}{4\pi |\mathbf{x} - \mathbf{x}'|} d^2x', \quad (55)$$

$$\mathbf{A}_N^{(1)} = \int_V \frac{\nabla' \times [q_N^{(1)}(\mathbf{x}') \hat{\mathbf{e}}_{r'}]}{4\pi |\mathbf{x} - \mathbf{x}'|} d^3x' + \oint_S \frac{[q_N^{(1)}(\mathbf{x}') \hat{\mathbf{e}}_{r'}] \times \hat{\mathbf{n}}'}{4\pi |\mathbf{x} - \mathbf{x}'|} d^2x'. \quad (56)$$

If $q_N^{(1)}$ decay rapidly enough as $|\mathbf{x}'|$ tends to infinity, then as the integral is extended to the entire space, the surface terms will vanish.

Consequently, we have

$$\begin{aligned} \mathbf{g}_Q &= \nu^{(0)} g_N^{(0)} \hat{\mathbf{e}}_r + \epsilon \left\{ \nu^{(0)} \left[\mathbf{g}_N^{(1)} + \mathcal{A}^{(0)} g_N^{(0)} g_{Nr}^{(1)} \hat{\mathbf{e}}_r \right] + \nabla \times \mathbf{A}_N^{(1)} \right\} + \mathcal{O}(\epsilon^2) \\ &= \nu^{(0)} g_N^{(0)} \hat{\mathbf{e}}_r - \epsilon \left\{ \nu^{(0)} \left[\nabla \Phi_N^{(1)} + \mathcal{A}^{(0)} \frac{dg_N^{(0)}}{dr} \Phi_N^{(1)} \hat{\mathbf{e}}_r \right] + \nabla \Upsilon_N^{(1)} \right\} + \mathcal{O}(\epsilon^2). \end{aligned} \quad (57)$$

The mass distribution is

$$4\pi G \rho^{(0)} = - \frac{1}{r^2} \frac{\partial r^2 g_N^{(0)}}{\partial r}, \quad (58)$$

and

$$4\pi G \rho^{(1)} = \nabla^2 \Phi_N^{(1)}. \quad (59)$$

4. An example

In this section, we present a simple example in AQUAL I.

First, it is interesting to point out the following:

- if $\Psi_{\text{N}}^{(1)}(r, \theta, \phi) = g_{\text{N}}^{(0)}(r)\psi_{\text{N}}^{(1)}(\theta, \phi)$ in AQUAL I or $\Phi_{\text{A}}^{(1)}(r, \theta, \phi) = g_{\text{A}}^{(0)}(r)\phi_{\text{A}}^{(1)}(\theta, \phi)$ in AQUAL II, then $\tilde{\mu}\mathbf{g}_{\text{A}} = \mathbf{g}_{\text{N}}$ or $\mathbf{g}_{\text{A}} = \tilde{\nu}\mathbf{g}_{\text{N}}$ up to first order (i.e., $\nabla \times \mathbf{h} = \mathcal{O}(\epsilon^2)$);
- if $\Psi_{\text{Q}}^{(1)}(r, \theta, \phi) = g_{\text{Q}}^{(0)}(r)\psi_{\text{Q}}^{(1)}(\theta, \phi)$ in QuMOND I or $\Phi_{\text{N}}^{(1)}(r, \theta, \phi) = g_{\text{N}}^{(0)}(r)\phi_{\text{N}}^{(1)}(\theta, \phi)$ in QuMOND II, then $\mu\mathbf{g}_{\text{Q}} = \mathbf{g}_{\text{N}}$ or $\mathbf{g}_{\text{Q}} = \nu\mathbf{g}_{\text{N}}$ up to first order (i.e., $\nabla \times \mathbf{A} = \mathcal{O}(\epsilon^2)$).

That is, if one of these conditions is satisfied, then the problem becomes similar to spherical ones. Moreover, the corresponding “deformation potential” of AQUAL I, $\Psi_{\text{N}}^{(1)}$, does not depend on the interpolation function if $\rho^{(1)}$ is given, see Equation (32). (From Equation (59), we note that if $\rho^{(1)}$ is given, then the “deformation potential” of QuMOND II, $\Phi_{\text{N}}^{(1)}$, does not depend on the interpolation function in general.)

For simplicity, we take the Bekenstein form $((\alpha, \eta) = (1, 0)$ in Equation (9)) in AQUAL I, and $\Psi_{\text{N}}^{(1)}(r, \theta, \phi) = g_{\text{N}}^{(0)}(r)\psi_{\text{N}}^{(1)}(\theta, \phi)$, then Equation (30) gives

$$g_{\text{Ar}} = \left(1 + x_{\text{N}}^{-1/2}\right)^{(0)} g_{\text{N}}^{(0)} - \epsilon \left(1 + \frac{1}{2}x_{\text{N}}^{-1/2}\right)^{(0)} \frac{dg_{\text{N}}^{(0)}}{dr} \psi_{\text{N}}^{(1)}, \quad (60)$$

$$g_{\text{A}\theta} = -\epsilon \left(1 + x_{\text{N}}^{-1/2}\right)^{(0)} \left(\frac{g_{\text{N}}^{(0)}}{r}\right) \frac{\partial \psi_{\text{N}}^{(1)}}{\partial \theta_1}, \quad (61)$$

$$g_{\text{A}\phi} = -\epsilon \left(1 + x_{\text{N}}^{-1/2}\right)^{(0)} \left(\frac{g_{\text{N}}^{(0)}}{r \sin \theta_1}\right) \frac{\partial \psi_{\text{N}}^{(1)}}{\partial \phi_1}. \quad (62)$$

The density is given by $4\pi G\rho = \nabla^2 \Phi_{\text{N}} = -\nabla \cdot (g_{\text{N}}^{(0)} \hat{\mathbf{e}}_r) + \epsilon \nabla^2 (g_{\text{N}}^{(0)} \psi_{\text{N}}^{(1)})$.

To educate ourselves, here is a simple example that gives a flattened axial symmetric mass distribution (oblate-like distribution: $\sin^2 \theta$),

$$g_{\text{N}}^{(0)} = -\frac{Gm_0}{r_0^2} \left(\frac{r}{r_0}\right)^p, \quad \psi_{\text{N}}^{(1)} = r_0 [p(p+1) \cos^2 \theta - (p^2 + p - 4)], \quad (63)$$

where $-2 < p < 0$. Substituting Equation (63) into Equations (60)–(62) explicitly provides \mathbf{g}_{A} , and the corresponding potential ($\mathbf{g}_{\text{A}} = -\nabla \Phi_{\text{A}}$)

$$\Phi_{\text{A}} = \frac{Gm_0}{r_0} \left\{ \left[\frac{1}{(p+1)} \left(\frac{r}{r_0}\right)^{(p+1)} + \frac{2}{(p+2)} \sqrt{\frac{a_0 r_0^2}{Gm_0}} \left(\frac{r}{r_0}\right)^{(p+2)/2} \right] \right\}$$

$$- \epsilon \left[\left(\frac{r}{r_0} \right)^p + \sqrt{\frac{a_0 r_0^2}{G m_0}} \left(\frac{r}{r_0} \right)^{p/2} \right] [p(p+1) \cos^2 \theta - (p^2 + p - 4)] \Bigg\}. \quad (64)$$

Putting $a_0 = 0$ in Equation (64) gives Φ_N . Moreover, the density is

$$\rho = \frac{m_0}{4\pi r_0^3} \left[(p+2) \left(\frac{r}{r_0} \right)^{p-1} + \epsilon p(p-2)(p+1)(p+3) \left(\frac{r}{r_0} \right)^{p-2} \sin^2 \theta \right]. \quad (65)$$

To ensure a positive density, we should take $\epsilon < 0$ for $-2 < p < -1$, and $\epsilon > 0$ for $-1 < p < 0$. Nevertheless, the model has the shortcoming that the density is dominated by the first-order term at small r .

Suppose the axis of symmetry is perpendicular to the line of sight. Set up a Cartesian coordinate system in the observer frame (ξ, η, ζ) such that the line of sight is along the ζ -axis, and the axis of symmetry of the object is along the ξ -axis. Thus, we have $r^2 = \xi^2 + \eta^2 + \zeta^2$ and $\cos \theta = \xi/r$, and

$$\begin{aligned} g_{A\xi} = & -\frac{Gm_0}{r_0^2} \left(\frac{\xi}{r} \right) \left\{ \left[\left(\frac{r}{r_0} \right)^p + \sqrt{\frac{a_0 r_0^2}{Gm_0}} \left(\frac{r}{r_0} \right)^{p/2} \right] \right. \\ & + \epsilon p \left[(p-3)(p+2) \left(\frac{r}{r_0} \right)^{p-1} + \frac{(p^2 - 3p - 8)}{2} \sqrt{\frac{a_0 r_0^2}{Gm_0}} \left(\frac{r}{r_0} \right)^{(p-2)/2} \right] \\ & \left. - \epsilon p(p+1) \left(\frac{\xi^2}{r^2} \right) \left[(p-2) \left(\frac{r}{r_0} \right)^{p-1} + \frac{(p-4)}{2} \sqrt{\frac{a_0 r_0^2}{Gm_0}} \left(\frac{r}{r_0} \right)^{(p-2)/2} \right] \right\}, \quad (66) \end{aligned}$$

$$\begin{aligned} g_{A\eta} = & -\frac{Gm_0}{r_0^2} \left(\frac{\eta}{r} \right) \left\{ \left[\left(\frac{r}{r_0} \right)^p + \sqrt{\frac{a_0 r_0^2}{Gm_0}} \left(\frac{r}{r_0} \right)^{p/2} \right] \right. \\ & + \epsilon p (p^2 + p - 4) \left[\left(\frac{r}{r_0} \right)^{p-1} + \frac{1}{2} \sqrt{\frac{a_0 r_0^2}{Gm_0}} \left(\frac{r}{r_0} \right)^{(p-2)/2} \right] \\ & \left. - \epsilon p(p+1) \left(\frac{\xi^2}{r^2} \right) \left[(p-2) \left(\frac{r}{r_0} \right)^{p-1} + \frac{(p-4)}{2} \sqrt{\frac{a_0 r_0^2}{Gm_0}} \left(\frac{r}{r_0} \right)^{(p-2)/2} \right] \right\}. \quad (67) \end{aligned}$$

For illustration purposes, we apply this model to strong gravitational lensing (see Appendix B). Figure 1 shows the critical curves and caustics for the case $p = -3/2$.

5. Summary and discussion

Non-spherical systems in the framework of MOND are a lot more difficult to analyse than spherical systems. There are plenty of astrophysical objects that can be approximated by a slightly deformed spherical distribution. As an alternative to dark matter, it is desirable to develop methods or algorithms to deal with such systems. Based on the compatibility condition, we propose a method to analyse slightly deformed spherical systems (i.e., slightly non-spherical systems) in the framework of MOND. There are two formulations of MOND, namely, AQUAL and QuMOND, and the compatibility condition can be written in two ways, and hence we have four different approaches, see Sections 3.1.1–3.2.2. In general, this involves solving the corresponding “deformation potential” when the mass distribution is given.

To examine the dynamics of an object, in principle, one requires observations of the distribution of its mass (e.g., brightness distribution) and the gravitational acceleration of the object (e.g., velocity distribution or light bending in gravitational lensing). For data fitting, one may start from a mass model and compute the gravitational acceleration, or the other way round. Here, we briefly summarise these two approaches in our proposed method.

(1) *Start from a model of mass distribution.*

Suppose we have a model of mass distribution $\rho = \rho^{(0)}(r) + \epsilon \rho^{(1)}(r, \theta, \phi)$, and a prescribed interpolation function, then we can deduce the gravitational acceleration as follows.

- AQUAL I with prescribed $\tilde{\nu}$
 - Equation (31) can be integrated to give the zeroth-order Newtonian acceleration $g_N^{(0)}$;
 - Equation (32) becomes a differential equation for the “deformation potential” $\Psi_N^{(1)}$;
 - once $\Psi_N^{(1)}$ is known, the MONDian acceleration \mathbf{g}_A is given by Equation (30).
- AQUAL II with prescribed $\tilde{\mu}$
 - Equation (40) can be integrated to give the zeroth-order MONDian acceleration $g_A^{(0)}$;
 - Equation (41) becomes a differential equation for the “deformation potential” $\Phi_A^{(1)}$;

– once $\Phi_A^{(1)}$ is known, the MONDian acceleration \mathbf{g}_A is given by Equation (33).

- QuMOND I with prescribed μ

– Equation (50) can be integrated to give the zeroth-order MONDian acceleration $g_Q^{(0)}$;

– Equation (51) becomes a differential equation for the “deformation potential” $\Psi_Q^{(1)}$;

– once $\Psi_Q^{(1)}$ is known, we can solve $\nabla^2 \varphi_Q^{(1)} = -\nabla \cdot [f_Q^{(1)} \hat{\mathbf{e}}_r]$ for $\varphi_Q^{(1)}$, where $f_Q^{(1)}$ is given by Equation (45);

– once $\Psi_Q^{(1)}$ and $\varphi_Q^{(1)}$ are known, the MONDian acceleration \mathbf{g}_Q is given by Equation (48).

- QuMOND II with prescribed ν

– Equation (58) can be integrated to give the zeroth-order Newtonian acceleration $g_N^{(0)}$;

– Equation (59) becomes a differential equation for the “deformation potential” $\Phi_N^{(1)}$;

– once $\Phi_N^{(1)}$ is known, we can solve $\nabla^2 \Upsilon_N^{(1)} = \nabla \cdot [q_N^{(1)} \hat{\mathbf{e}}_r]$ for $\Upsilon_N^{(1)}$, where $q_N^{(1)}$ is given by Equation (54);

– once $\Phi_N^{(1)}$ and $\Upsilon_N^{(1)}$ are known, the MONDian acceleration \mathbf{g}_A is given by Equation (57).

(2) *Start from a model of gravitational acceleration.*

If we start from a model of acceleration $\mathbf{g} = g^{(0)}(r) \hat{\mathbf{e}}_r + \epsilon \mathbf{g}^{(1)}(r, \theta, \phi)$, and a prescribed interpolation function, then we can deduce the mass distribution. However, in general, there is no guarantee that the deduced density is non-negative everywhere.

- AQUAL (either I or II) with prescribed $\tilde{\mu}$

– the density is given by $4\pi G\rho = -\nabla \cdot (\tilde{\mu}\mathbf{g})$.

- QuMOND I with prescribed μ

– set $g_Q^{(0)} = g^{(0)}$, then the zeroth-order density $\rho^{(0)}$ is given by Equation (50);

– Equation (43) gives $\nabla \cdot \mathbf{F}_Q^{(1)} = \nabla \cdot \mathbf{g}^{(1)}$;

- this equation together with Equation (45) give a differential equation for the “deformation potential” $\Psi_{\text{Q}}^{(1)}$;
- once $\Psi_{\text{Q}}^{(0)}$ is known, the first-order density $\rho^{(1)}$ is given by Equation (51).
- QuMOND II with prescribed ν
 - solve $\nu^{(0)}g_{\text{N}}^{(0)} = g^{(0)}$ for $g_{\text{N}}^{(0)}$ (or $g_{\text{N}}^{(0)} = \mu^{(0)}g^{(0)}$ if μ is given);
 - the zeroth-order density $\rho^{(0)}$ is the given by Equation (58);
 - $\nabla \cdot \mathbf{g}_{\text{Q}}^{(1)} = \nabla \cdot \mathbf{g}^{(1)}$ together with Equation (57) give a differential equation for the “deformation potential” $\Phi_{\text{N}}^{(1)}$;
 - once $\Phi_{\text{N}}^{(1)}$ is known, the first-order density $\rho^{(1)}$ is given by Equation (59).

In most cases, we will follow the first procedure as it is rather straightforward to model the mass distribution from the surface brightness distribution.

For some specific forms of the deformation potential, e.g., $\Psi_{\text{N}}^{(1)}(r, \theta, \phi) = g_{\text{N}}^{(0)}(r)\psi_{\text{N}}^{(1)}(\theta, \phi)$ in AQUAL I, $\Phi_{\text{A}}^{(1)}(r, \theta, \phi) = g_{\text{A}}^{(0)}(r)\phi_{\text{A}}^{(1)}(\theta, \phi)$ in AQUAL II, $\Psi_{\text{Q}}^{(1)}(r, \theta, \phi) = g_{\text{Q}}^{(0)}(r)\psi_{\text{Q}}^{(1)}(\theta, \phi)$ in QuMOND I, or $\Phi_{\text{N}}^{(1)}(r, \theta, \phi) = g_{\text{N}}^{(0)}(r)\phi_{\text{N}}^{(1)}(\theta, \phi)$ in QuMOND II, the Newtonian and MONDian gravitational accelerations are in the same direction (up to first order in ϵ), i.e., $\mathbf{g}_{\text{A}} \parallel \mathbf{g}_{\text{N}}$, or $\mathbf{g}_{\text{Q}} \parallel \mathbf{g}_{\text{N}}$. Spherical systems have the same property.

We would like to point out an attractive feature of QuMOND II. For a prescribed $\rho^{(1)}$ the “deformation potential” $\Phi_{\text{N}}^{(1)}$ of QuMOND II does not depend on the interpolation function. A similar feature occurs in AQUAL I, but only if the condition $\Psi_{\text{N}}^{(1)}(r, \theta, \phi) = g_{\text{N}}^{(0)}(r)\psi_{\text{N}}^{(1)}(\theta, \phi)$ is satisfied (see Equation (32)).

As an alternative to the dark matter paradigm, many of MOND’s studies were devoted to galaxy systems. The luminous parts of these systems (either elliptical galaxies, spiral galaxies, or clusters of galaxies), in general, are asymmetric. The procedure described above provides a tool enabling us to analyse many aspherical systems in the framework of MOND (it cannot address every asymmetric configuration though). The method is flexible enough for us to perform some serious modelling on the (baryonic) mass distribution of galaxy systems (in particular, elliptical galaxies) when we study phenomena such as gravitational lensing and stellar dynamics in these systems.

Cold dark matter simulations showed that the shape of the dark matter haloes is in generally aspherical (their orientations with respect to the baryonic matter in galaxies are studied as well; see, e.g., Jing & Suto 2002; Springel et al. 2005; Hayashi et al. 2007;

Vera-Ciro et al. 2011, 2014; Schneider et al. 2012; Velliscig et al. 2015; Gerhard 2013). Observations such as gravitational lensing, or stellar and satellites kinematics, may place constraints on the shape of the haloes and the corresponding gravitational field (e.g., Bailin et al. 2008; Howell & Brainerd 2010; Deason et al. 2011; Bett 2012; van Uitert et al. 2012; Hayashi & Chiba 2012, 2014, 2015; Vera-Ciro & Helmi 2013; Joachimi et al. 2013a,b; Schrabback et al. 2015). These observations also place constraints on MOND as well. The MONDian gravitational field is dictated by ρ_b , the shape and mass distribution of the baryons in the galaxy (the luminous part of the galaxy). Suppose a Newtonian field equivalent to the MONDian field is produced by an effective total mass ρ'_t , then $\rho'_{DM} = \rho'_t - \rho_b$ can be called the effective dark matter distribution. In QuMOND formulation, the expression for the effective dark matter distribution is simple, as it involves the Newtonian field from the baryons only:

$$4\pi G\rho'_{DM,Q} = -\frac{d\nu}{d|\mathbf{g}_N|} \mathbf{g}_N \cdot \nabla |\mathbf{g}_N|, \quad (68)$$

where $\nabla \cdot \mathbf{g}_N = -4\pi G\rho_b$, and ν depends on $|\mathbf{g}_N|$. In the AQUAL formulation

$$4\pi G\rho'_{DM,A} = \frac{d\tilde{\mu}}{d|\mathbf{g}_A|} \mathbf{g}_A \cdot \nabla |\mathbf{g}_A|, \quad (69)$$

where \mathbf{g}_A and \mathbf{g}_N are related by Equation (6) or (7), and $\tilde{\mu}$ depends on $|\mathbf{g}_A|$. Observations will place a constraint on the interpolation function $\tilde{\mu}(|\mathbf{g}_A|/a_0)$ or $\nu(|\mathbf{g}_N|/a_0)$, and may even distinguish between AQUAL and QuMOND.

As illustrated in Section 4 (and Appendix B), strong gravitational lensing will be a straightforward application of the method presented in this article. A deformed spherical lens can be used to study arcs, rings, quadruple-image systems in gravitational lens surveys, such as CASTLES, SLACS, Master Lens, SQLS, CLASS, CLASH, GLASS, etc.. In particular, quadruple-image systems with high-quality data are nice targets, such as B1422+231 (Nierenberg et al. 2014), B1608+656 (Suyu et al. 2009), HE0435-1223 (Kochanek et al. 2006), MGJ0414+0534 (Trotter et al. 2000), and PG1115+080 (Impry et al. 1998). The results will place some constraints on the parameters in MOND and/or the Hubble constant. We will consider analysis of these systems elsewhere.

The author is grateful to Yong Tian and Mu-Chen Chiu for stimulating discussions on the development of this work. This work is supported in part by the Taiwan Ministry of Science and Technology, grants MOST 102-2112-M-008-019-MY3 and MOST 104-2923-M-008-001-MY3.

A. Gravitational redshift

In this appendix, we use simple estimates to place some constraint on the MOND interpolation function $\tilde{\mu}(x)$ or its inverse $\tilde{\nu}(x_N)$ by the gravitational redshift measurement from a tabletop atomic interferometer experiment (Müller et al. 2010).

Assuming that the Earth is a sphere, we have for AQUAL $\tilde{\mu}(x_A)\nabla\Phi_A = \nabla\Phi_N$ and $\nabla\Phi_A = \tilde{\nu}(x_N)\nabla\Phi_N$ (see Equation (12)), and for QuMOND $\nu(x_N)\nabla\Phi_N = \nabla\Phi_Q$ and $\nabla\Phi_N = \mu(x_Q)\nabla\Phi_Q$ (see Equation (19)). Here, $x_N = |\nabla\Phi_N|/a_0$, $x_A = |\nabla\Phi_A|/a_0$ and $x_Q = |\nabla\Phi_Q|/a_0$. The accumulated phase due to redshift can be expressed as (see Müller et al. 2010)

$$\Delta\phi \approx -\frac{\omega_C}{c^2} \int z\hat{e}_r \cdot \nabla\Phi_A(r_E) dt = -\frac{\omega_C}{c^2} \int \tilde{\nu}z\hat{e}_r \cdot \nabla\Phi_N(r_E) dt, \quad (\text{A1})$$

for AQUAL. Here, $\omega_C = mc^2/\hbar$ is the Compton wavelength of the atom, r_E is the radius of the Earth, and $r = r_E + z$ ($z \ll r_E$). If we replace Φ_A and $\tilde{\nu}$ by Φ_Q and ν in Equation (A1), then we obtain the corresponding expression for QuMOND.

The parameter used to model the anomalies in gravitational redshift in Müller et al. (2010) is

$$\beta = \tilde{\nu}(x_N) - 1 = \left[1 + \frac{1}{2} \left(\sqrt{4\chi_N^{-\alpha} + \eta^2} - \eta \right) \right]^{1/\alpha} - 1, \quad (\text{A2})$$

where we adopted the inverted interpolation function (Equation (9); note that $\alpha > 0$ and $\eta \geq 0$). Supposing that this canonical form is valid in the high acceleration regime (i.e., the Newtonian limit, $x_N \gg 1$, $\tilde{\nu} - 1 \ll 1$), then the experiment by Müller et al. (2010) would place some constraint on the canonical form. Often, an upper bound of β is obtained in gravitational redshift experiments. Equation (A2) thus gives a constraint on (α, η) ,

$$\eta > \frac{x_N^{-\alpha} - [(1 + \beta_u)^\alpha - 1]^2}{[(1 + \beta_u)^\alpha - 1]}, \quad (\text{A3})$$

where β_u is the observed upper bound of β .

In the atomic interferometer experiment, Müller et al. (2010) obtained $\beta_u = 7 \times 10^{-9}$. If we take the nominal value of gravitational acceleration on Earth's surface $|\nabla\Phi_N(r_E)| = 9.81 \text{ m s}^{-2}$ and the acceleration constant $a_0 = 1.2 \times 10^{-10} \text{ m s}^{-2}$ (e.g., Sanders & McGaugh 2002), then we have $x_N = 8.175 \times 10^{10}$. Figure 2 shows the constraint on the parameter space (α, η) . The white (gray) region in the figure is the parameter space that is consistent with (excluded by) the experiment. For instance, for $\eta = 0$, α must be larger than 1.464; and for $\alpha = 1$, η must be larger than 0.001747.

B. Lens equation

In this appendix, we write down the lens equation for the example in Section 4. Assuming a small angle of deflection, the lens equation is

$$\vec{\beta} = \vec{\vartheta} + \frac{2D_{\text{LS}}}{c^2 D_{\text{S}}} \int \mathbf{g}_{\perp} d\zeta, \quad (\text{B1})$$

where $\vec{\beta}$ and $\vec{\vartheta}$ are the position angle of the source and image, respectively. D_{LS} and D_{S} are the distances of the source from the lens and from the observer, respectively. Here, the integration is taken along the undeflected path ζ from the source to the observer (which can be consider as from negative infinity to positive infinity). \mathbf{g}_{\perp} is the gravitational acceleration perpendicular to this path. \mathbf{g}_{\perp} is a function of (ξ, η, ζ) , and $\xi \approx D_{\text{L}}\vartheta_{\xi}$, $\eta \approx D_{\text{L}}\vartheta_{\eta}$, where D_{L} is the distance between the lens and the observer. Substituting Equations (66) and (67) into Equation (B1), we get (with $\vartheta^2 = \vartheta_{\xi}^2 + \vartheta_{\eta}^2$)

$$\begin{aligned} \beta_{\xi} = & \vartheta_{\xi} - \frac{\vartheta_{\text{E}}^2 \vartheta_{\xi}}{\vartheta_{\text{m}}^2} \left\{ \frac{\vartheta^p}{\vartheta_{\text{m}}^p} \left[\mathcal{J}_1 + \frac{\epsilon \vartheta_{\text{m}}}{\vartheta} \left(\mathcal{J}_5 - \frac{\vartheta_{\xi}^2}{\vartheta^2} \mathcal{J}_3 \right) \right] \right. \\ & \left. + \frac{\vartheta_{\text{m}}}{\vartheta_0} \frac{\vartheta^{p/2}}{\vartheta_{\text{m}}^{p/2}} \left[\mathcal{J}_2 + \frac{\epsilon \vartheta_{\text{m}}}{\vartheta} \left(\mathcal{J}_6 - \frac{\vartheta_{\xi}^2}{\vartheta^2} \mathcal{J}_4 \right) \right] \right\}, \end{aligned} \quad (\text{B2})$$

$$\begin{aligned} \beta_{\eta} = & \vartheta_{\eta} - \frac{\vartheta_{\text{E}}^2 \vartheta_{\eta}}{\vartheta_{\text{m}}^2} \left\{ \frac{\vartheta^p}{\vartheta_{\text{m}}^p} \left[\mathcal{J}_1 + \frac{\epsilon \vartheta_{\text{m}}}{\vartheta} \left(\mathcal{J}_7 - \frac{\vartheta_{\xi}^2}{\vartheta^2} \mathcal{J}_3 \right) \right] \right. \\ & \left. + \frac{\vartheta_{\text{m}}}{\vartheta_0} \frac{\vartheta^{p/2}}{\vartheta_{\text{m}}^{p/2}} \left[\mathcal{J}_2 + \frac{\epsilon \vartheta_{\text{m}}}{\vartheta} \left(\mathcal{J}_8 - \frac{\vartheta_{\xi}^2}{\vartheta^2} \mathcal{J}_4 \right) \right] \right\}, \end{aligned} \quad (\text{B3})$$

where

$$\vartheta_{\text{E}}^2 = \frac{4Gm_0 D_{\text{LS}}}{c^2 D_{\text{S}} D_{\text{L}}}, \quad \vartheta_0^2 = \frac{Gm_0}{D_{\text{L}}^2 a_0}, \quad \vartheta_{\text{m}} = \frac{r_0}{D_{\text{L}}}, \quad (\text{B4})$$

$$\mathcal{J}_1 = \mathcal{I}_{(1-p)/2}, \quad (\text{B5})$$

$$\mathcal{J}_2 = \mathcal{I}_{(2-p)/4}, \quad (\text{B6})$$

$$\mathcal{J}_3 = p(p-2)(p+1) \mathcal{I}_{(4-p)/2}, \quad (\text{B7})$$

$$\mathcal{J}_4 = \frac{1}{2} p(p-4)(p+1) \mathcal{I}_{(8-p)/4}, \quad (\text{B8})$$

$$\mathcal{J}_5 = p(p-3)(p+2) \mathcal{I}_{(2-p)/2}, \quad (\text{B9})$$

$$\mathcal{J}_6 = \frac{1}{2} p(p^2 - 3p - 8) \mathcal{I}_{(4-p)/4}, \quad (\text{B10})$$

$$\mathcal{J}_7 = p(p^2 + p - 4) \mathcal{I}_{(2-p)/2}, \quad (\text{B11})$$

$$\mathcal{J}_8 = \frac{1}{2} p(p^2 + p - 4) \mathcal{I}_{(4-p)/4}. \quad (\text{B12})$$

Here,

$$\begin{aligned}
\mathcal{I}_q &= \frac{1}{2} \int_{-\tilde{D}_{\text{LS}}}^{\tilde{D}'_{\text{L}}} \frac{d\tilde{\zeta}}{(1+\tilde{\zeta}^2)^q} = \frac{1}{2} \int_0^{\tilde{D}'_{\text{L}}} \frac{d\tilde{\zeta}}{(1+\tilde{\zeta}^2)^q} + \frac{1}{2} \int_0^{\tilde{D}_{\text{LS}}} \frac{d\tilde{\zeta}}{(1+\tilde{\zeta}^2)^q} \\
&= \frac{1}{2} \left[\tilde{\zeta} {}_2F_1 \left(\frac{1}{2}, q, \frac{3}{2}, -\tilde{\zeta}^2 \right) \right]_0^{\tilde{D}'_{\text{L}}} + \frac{1}{2} \left[\tilde{\zeta} {}_2F_1 \left(\frac{1}{2}, q, \frac{3}{2}, -\tilde{\zeta}^2 \right) \right]_0^{\tilde{D}_{\text{LS}}} \\
&\approx \frac{\Gamma(\frac{1}{2}-q)}{4\Gamma(\frac{3}{2}-q)} \left(\tilde{D}'_{\text{L}}{}^{1-2q} + \tilde{D}_{\text{LS}}{}^{1-2q} \right) + \frac{\sqrt{\pi}\Gamma(q-\frac{1}{2})}{2\Gamma(q)} + \dots, \tag{B13}
\end{aligned}$$

where $\tilde{\zeta} = \zeta/\sqrt{\xi^2 + \eta^2}$, $\tilde{D}'_{\text{L}} = D'_{\text{L}}/\sqrt{\xi^2 + \eta^2}$ and $\tilde{D}_{\text{LS}} = D_{\text{LS}}/\sqrt{\xi^2 + \eta^2}$, and note that $\tilde{D}'_{\text{L}}, \tilde{D}_{\text{LS}} \gg 1$. For $q > \frac{1}{2}$, the first term in Equation (B13) is subordinate to the second term and can be neglected. As we are only interested in $-2 < p < 0$, all \mathcal{J} s satisfy $q > \frac{1}{2}$.

Equations (B2) and (B3) are the mapping of the image to the source. The determinant of the inverse of the Jacobian of the mapping gives the magnification of the image. The positions of the image when the magnification becomes infinite form the so called critical lines. The corresponding source positions form caustics.

For completeness, we write down the time-delay function:

$$\Delta T = \frac{(1+z_{\text{L}})D_{\text{L}}D_{\text{S}}}{c} \frac{1}{D_{\text{LS}}} \left[\frac{1}{2} \left(\vec{\theta} - \vec{\beta} \right)^2 - \psi \right], \tag{B14}$$

where $\psi = 2D_{\text{LS}}/(c^2D_{\text{L}}D_{\text{S}}) \int_{-D_{\text{LS}}}^{D'_{\text{L}}} \Phi d\zeta$. Taking Φ_{A} in Equation (64) as Φ , we have

$$\begin{aligned}
\psi &= \vartheta_{\text{E}}^2 \left\{ \frac{\vartheta^{p+2}}{\vartheta_{\text{m}}^{p+2}} \left[\mathcal{J}_9 + \frac{\epsilon \vartheta_{\text{m}}}{\vartheta} \left(\mathcal{J}_{13} - \frac{\vartheta_{\xi}^2}{\vartheta^2} \mathcal{J}_{11} \right) \right] \right. \\
&\quad \left. + \frac{\vartheta_{\text{m}}}{\vartheta_0} \frac{\vartheta^{(p+4)/2}}{\vartheta_{\text{m}}^{(p+4)/2}} \left[\mathcal{J}_{10} + \frac{\epsilon \vartheta_{\text{m}}}{\vartheta} \left(\mathcal{J}_{14} - \frac{\vartheta_{\xi}^2}{\vartheta^2} \mathcal{J}_{12} \right) \right] \right\}, \tag{B15}
\end{aligned}$$

where

$$\mathcal{J}_9 = \frac{1}{(p+1)} \mathcal{I}_{-(1+p)/2}, \tag{B16}$$

$$\mathcal{J}_{10} = \frac{2}{(p+2)} \mathcal{I}_{-(2+p)/4}, \tag{B17}$$

$$\mathcal{J}_{11} = p(p+1) \mathcal{I}_{(2-p)/2}, \tag{B18}$$

$$\mathcal{J}_{12} = p(p+1) \mathcal{I}_{(4-p)/4}, \tag{B19}$$

$$\mathcal{J}_{13} = (p^2 + p - 4) \mathcal{I}_{-p/2}, \tag{B20}$$

$$\mathcal{J}_{14} = (p^2 + p - 4) \mathcal{I}_{-p/4}. \tag{B21}$$

Moreover, the projected surface density $\Sigma = \int_{-\infty}^{\infty} \rho d\zeta$ is

$$\Sigma = \frac{m_0}{2\pi r_0^2} \frac{\vartheta^p}{\vartheta_m^p} \left\{ (p+2) \mathcal{I}_{(1-p)/2} + \frac{\epsilon \vartheta_m}{\vartheta} p(p-2)(p+1)(p+3) \left[\mathcal{I}_{(2-p)/2} - \frac{\vartheta_\xi^2}{\vartheta^2} \mathcal{I}_{(4-p)/2} \right] \right\}. \quad (\text{B22})$$

REFERENCES

- Aguirre, A., Schaye, J., & Quataert, E. 2001, *ApJ*, 561, 550
- Angus, G. W. 2009, *MNRAS*, 394, 527
- Angus, G.W., Famaey, B., & Zhao, H.S. 2006, *MNRAS*, 371, 138
- Angus, G.W., & McGaugh, S.S. 2008, *MNRAS*, 383, 417
- Angus, G.W., van der Heyden, K.J., Famaey, B., et al. 2012, *MNRAS*, 421, 2598
- Angus, G.W., Gentile, G., Diaferio, A., et al. 2014, *MNRAS*, 440, 746
- Bailin, J., Power, C., & Norberg, P. 2008, *MNRAS*, 390, 1133
- Baumgardt, H., Grebel, E.K., & Kroupa, P. 2005, *MNRAS*, 359, L1
- Begeman, K.G., Broeils, A.H., & Sanders, R.H. 1991, *MNRAS*, 249, 523
- Bekenstein, J.D. 2004, *Phys. Rev. D*, 70, 083509
- Bekenstein, J.D., & Milgrom, M. 1984, *ApJ*, 286, 7
- Bekenstein, J.D., & Sanders, R.H. 2012, *MNRAS*, 421, L59
- Bett, P. 2012, *MNRAS*, 420, 3303
- Blanchet, L., & Novak, J. 2011, *MNRAS*, 412, 2530
- Bourliot, F., Ferreira, P.G., Mota, D.F., & Skordis, C. 2007, *Phys. Rev. D*, 75, 063508
- Brada, R., & Milgrom, M. 1995, *MNRAS*, 276, 453
- Brada, R., & Milgrom, M. 1999, *ApJ*, 519, 590
- Brada, R., & Milgrom, M. 2000a, *ApJ*, 531, L21
- Brada, R., & Milgrom, M. 2000b, *ApJ*, 541, 556

- Candlish, G.N., Smith, R., & Fellhauer, M. 2015, MNRAS, 446, 1060
- Chae, K.H., & Gong, I.T. 2015, MNRAS, 451, 1719
- Chiu, M.C., Ko, C.M., & Tian, Y. 2006, ApJ, 636, 565
- Chiu, M.C., Ko, C.M., Tian, Y., & Zhao, H. 2011, Phys. Rev. D, 83, 063523
- Ciotti, L., Londrillo, P., & Nipoti, C. 2006, ApJ, 640, 741
- Ciotti, L., Zhao, H.S., & de Zeeuw, P.T. 2012, MNRAS, 422, 2058
- Clifton, T., & Zlosnik, T.G. 2010, Phys. Rev. D, 81, 103525
- Clowe, D., Gonzalez, A.H., & Markevitch, M. 2003, ApJ, 604, 596
- Contaldi, C.R., Wiseman, T., & Withers, B. 2008, Phys. Rev. D, 78, 044034
- de Blok, W.J.G., & McGaugh, S.S. 1998, ApJ, 508, 132
- Deason, A.J., McCarthy, I.G., Font, A.S., et al. 2011, MNRAS, 415, 2607
- Derakhshani, K. 2014, ApJ, 783, 48
- Dodelson, S., & Liguori, M. 2006, Phys. Rev. Lett., 97, 231301
- Famaey, B., & Binney, J. 2005, MNRAS, 363, 603
- Famaey, B., & McGaugh, S.S. 2012, Living Rev. Relativity, 15, (2012), 10
- Famaey, B., & McGaugh, S.S. 2013, J. Phys. Conference Series, 437, 012001
- Feix, M., Fedeli, C., & Bartelmann, M. 2008, A&A, 480, 313
- Gentile, G., Famaey, B., Combes, F., et al. 2007, A&A, 472, L25
- Gerhard, O. 2013, Proc. IAUS 295: The intriguing life of massive galaxies, ed. D. Thomas, A. Pasquali & I. Ferreras, pp.211
- Haghi, H., Baumgardt, H., & Kroupa, P. 2011, A&A, 527, A33
- Haghi, H., Baumgardt, H., Kroupa, P., et al. 2009, MNRAS, 395, 1549
- Hayashi, E., Navarro, J.F., & Springel, V. 2007, MNRAS, 377, 50
- Hayashi, K., & Chiba, M. 2012, ApJ, 755, 145

- Hayashi, K., & Chiba, M. 2014, *ApJ*, 489, 62
- Hayashi, K., & Chiba, M. 2015, *ApJ*, 810, 22
- Hees, A., Famaey, B., Angus, G.W., & Gentile, G. 2016, *MNRAS*, 455, 449
- Hees, A., Folkner, W.M., Jacobson, R.A., & Park, R.S. 2014, *Phys. Rev. D*, 89, 102002
- Hohensee, M., Chu, S., Peters, A., & Müller, H. 2011, *Phys. Rev. Lett.*, 106, 151102
- Howell, P.J., & Brainerd, T.G. 2010, *MNRAS*, 407, 891
- Impey, C.D., Falco, E.E., Kochanek, C.S., et al. 1998, *ApJ*, 509, 551
- Iorio, L. 2008, *J. Grav. Phys.*, 2, 26
- Iorio, L. 2009, *Ap&SS*, 323, 215
- Iorio, L. 2010a, *Open Astron. J.*, 3, 1
- Iorio, L. 2010b, *Open Astron. J.*, 3, 156
- Iorio, L. 2013, *Class. Quantum Grav.*, 30, 165018
- Jing, Y.P., & Suto, Y. 2002, *ApJ*, 574, 538
- Joachimi, B., Semboloni, E., Bett, P.E., et al. 2013a, *MNRAS*, 431, 477
- Joachimi, B., Semboloni, E., Hilbert, S., et al. 2013b, *MNRAS*, 436, 819
- Klypin, A., & Prada, F. 2009, *ApJ*, 690, 1488
- Kochanek, C.S., Morgan, N.D., Falco, E.E., et al. 2006, *ApJ*, 640, 47
- Llinares, C., Knebe, A., & Zhao, H.S. 2008, *MNRAS*, 391, 1778
- Londrillo, P., & Nipoti, C. 2009, *Mem. S.A.It. Suppl.*, 13, 89
- Lüghausen, F., Famaey, B., & Kroupa, P. 2014, *MNRAS*, 441, 2497
- Lüghausen, F., Famaey, B., & Kroupa, P. 2015, *Canadian J. Phys.*, 93, 232
- McGaugh, S.S. 2005, *ApJ*, 632, 859
- McGaugh, S.S. 2011, *Phys. Rev. Lett.*, 106, 121303
- McGaugh, S.S. 2012, *AJ*, 143, 40

- McGaugh, S.S. 2015, *Can. J. Phys.*, 93, 250
- McGaugh, S.S., & Milgrom, M. 2013a, *ApJ*, 766, 22
- McGaugh, S.S., & Milgrom, M. 2013b, *ApJ*, 775, 139
- Milgrom, M. 1983a, *ApJ*, 270, 365
- Milgrom, M. 1983b, *ApJ*, 270, 371
- Milgrom, M. 1983c, *ApJ*, 270, 384
- Milgrom, M. 1986, *ApJ*, 302, 617
- Milgrom, M. 2009a, *Phys. Rev. D*, 80, 123536
- Milgrom, M. 2009b, *MNRAS*, 399, 474
- Milgrom, M. 2010a, *MNRAS*, 403, 886
- Milgrom, M. 2010b, *Phys. Rev. D*, 82, 043523
- Milgrom, M. 2012a, *Phys. Rev. Lett.*, 109, 131101
- Milgrom, M. 2012b, *MNRAS*, 426, 673
- Milgrom, M. 2013, *Phys. Rev. Lett.*, 111, 041105
- Milgrom, M., & Sanders, R.H. 2003, *ApJ*, 599, L25
- Milgrom, M., & Sanders, R.H. 2007, *ApJ*, 658, L17
- Müller, H., Peters, A., & Chu, S. 2010, *Nature*, 463, 926
- Nierenberg, A.M., Treu, T., Wright, S.A., et al. 2014, *MNRAS*, 442, 2434
- Nipoti, C., Londrillo, P., & Ciotti, L. 2007a, *ApJ*, 660, 256
- Nipoti, C., Londrillo, P., & Ciotti, L. 2007b, *MNRAS*, 381, L104
- Nipoti, C., Ciotti, L., Binney, J., & Londrillo, P. 2008, *MNRAS*, 386, 2194
- Nipoti, C., Ciotti, L., & Londrillo, P. 2011, *MNRAS*, 414, 3298
- Sanders, R.H. 1996, *ApJ*, 473, 117
- Sanders, R.H. 2003, *MNRAS*, 342, 901

- Sanders, R.H. 2006, MNRAS, 370, 1519
- Sanders, R.H. 2010a, *The Dark Matter Problem: A Historical Perspective* (Cambridge: Cambridge Univ. Press)
- Sanders, R.H. 2010b, MNRAS, 407, 1128
- Sanders, R.H. 2014, MNRAS, 439, 1781
- Sanders, R.H., & McGaugh, S.S. 2002, ARA&A, 40, 263
- Sanders, R.H., & Noordermeer, E. 2007, MNRAS, 379, 702
- Sanders, R.H., & Verheijen, M.A.W. 1998, ApJ, 503, 97
- Schneider, M.D., Frenk, C.S., & Cole, S. 2012, JCAP, 05, 030
- Schrabback, T., Hilbert, S., Hoekstra, H., et al. 2015, MNRAS, 454, 1432
- Seifert, M.D. 2007, Phys. Rev. D, 76, 064002
- Sereno, M. & Jetzer, Ph. 2006, MNRAS, 371, 626
- Shan, H.Y., Feix, M., Famaey, B., & Zhao, H.S. 2008, MNRAS, 387, 1303
- Skordis, C. 2006, Phys. Rev. D, 74, 103513
- Skordis, C. 2008, Phys. Rev. D, 77, 123502
- Skordis, C. 2009, CQGra, 26, 143001
- Skordis, C., Mota, D.F., Ferreira, P.G., & Boehm, C. 2006, Phys. Rev. Lett., 96, 011301
- Sokaliwska, M., Fahr, H.J., & Kroupa, P. 2010, MNRAS, 407, 2557
- Springel, V., White, S.D.M., Jenkins, A., et al. 2005, Nature, 435, 629
- Suyu, S.H., Marshall P.J., Blandford, R.D., et al. 2009, ApJ, 691, 277
- Swaters, R.A., Sanders, R.H., & McGaugh, S.S. 2010, ApJ, 718, 380
- Tian, Y., Ko, C.M., & Chiu, M.C. 2013, ApJ, 770, 154
- Tian, Y., & Ko, C.M. 2015, ApJ, submitted
- Tiret, O., & Combes, F. 2007, A&A, 464, 517

- Tiret, O., & Combes, F. 2008, *A&A*, 483, 719
- Trotter, C.S., Winn, J.N., & Hewitt, J.N. 2000, *ApJ*, 535, 671
- van Uitert, E., Hoekstra, H., Schrabback, T., 2012, *A&A*, 545, A71
- Vera-Ciro, C.A., Sales, L.V., Helmi, A., et al. 2011, *MNRAS*, 416, 1377
- Vera-Ciro, C.A., & Helmi, A. 2013, *ApJ*, 733, L4
- Vera-Ciro, C.A., Sales, L.V., Helmi, A., & Navarro, J.F. 2014, *MNRAS*, 439, 2863
- Velliscig, M., Cacciato, M., Schaye, J., et al. 2015, *MNRAS*, 453, 721
- Wang, Y., Wu, X., & Zhao, H.S. 2008, *ApJ*, 677, 1033
- Wojtak, R., Hansen, S.H., & Hjorth, J. 2011, *Nature*, 477, 567
- Wu, X., Zhao, H.S., Famaey, B., et al. 2007, *ApJ*, 665, L101
- Wu, X., Zhao, H.S., Wang, Y., et al. 2009, *MNRAS*, 396, 109
- Zhao, H.S., Bacon, D.J., Taylor, A.N., & Horne, K. 2006, *MNRAS*, 368, 171

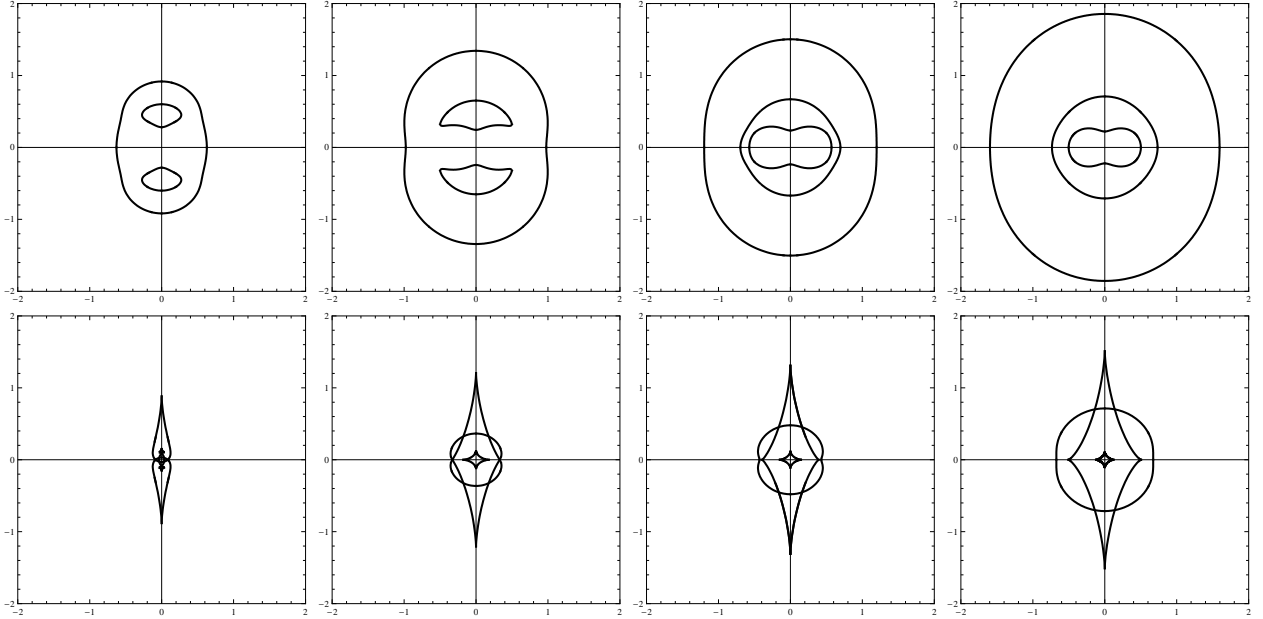


Fig. 1.— Example of strong gravitational lensing in AQUAL I. Critical curves and caustics for the case $p = -3/2$ (i.e., $g_N^{(0)} \propto r^{-3/2}$). The upper row is the critical curves and the lower row is the caustics. From left to right the parameters $(\epsilon, \vartheta_E, \vartheta_0)$ for the columns are $(-0.1, 1, \infty)$, $(-0.1, 1, 4)$, $(-0.1, 1, 3)$, and $(-0.1, 1, 2)$. The definitions of the parameters are given in Appendix B. ϑ_0 represents the ratio of the characteristic acceleration of the system to a_0 . The larger is ϑ_0 the closer is the system to the Newtonian regime (cf. x_A in Equation (1)). The plots are in units of $\vartheta_m = r_0/D_L$ (D_L is the distance between the lens and the observer).

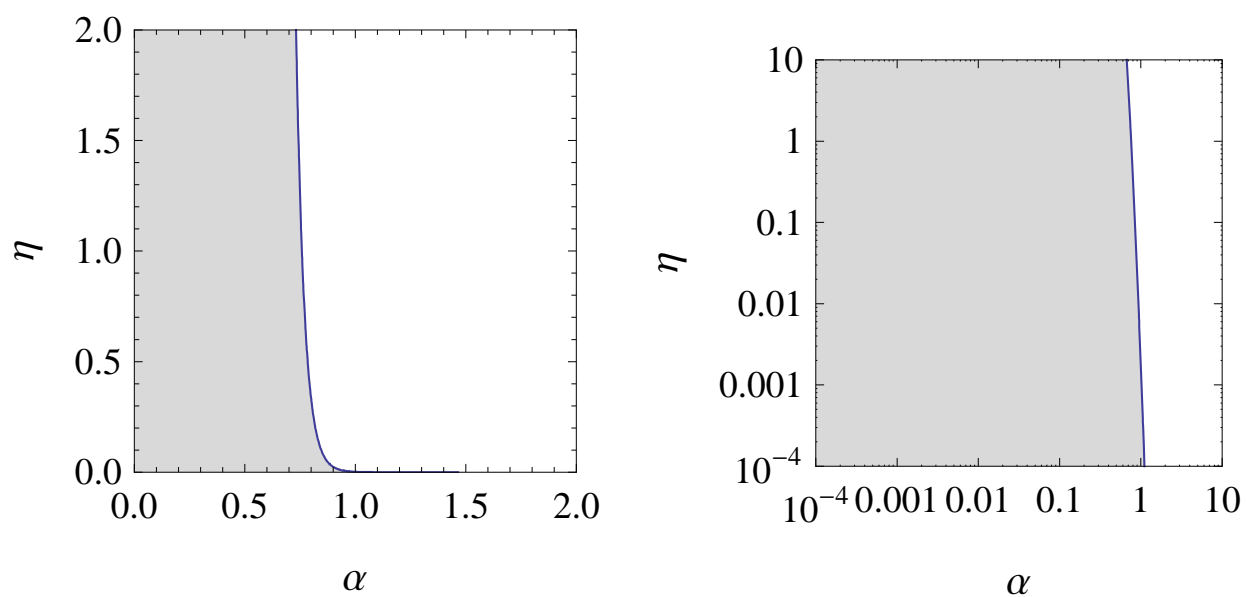


Fig. 2.— Constraint on the form of the MOND interpolation function by the atomic interferometer gravitational redshift experiment (Müller et al. 2010). α and η are the parameters in a canonical form of the interpolation function (see Equation (9)). The left panel is a linear plot while the right panel is a log-log plot. The white region is allowed by the experiment and the gray region is excluded.